Supplementary Material

Simultaneous Fat Saturation and Magnetization Transfer Contrast Imaging with Steady-State Incoherent Sequences

FENG ZHAO*,[1],JON-FREDRIK NIELSEN[1], SCOTT D. SWANSON[2], JEFFREY A. FESSLER[3] AND DOUGLAS C. NOLL[1]

[1]Biomedical Engineering Department, [2] Radiology Department, and [3] Department of Electrical Engineering and Computer Science, The University of Michigan, Ann Arbor, MI, USA

INTRODUCTION

This is the supplementary material for the paper "Simultaneous Fat Saturation and Magnetization Transfer Contrast Imaging with Steady-State Incoherent Sequences". In this material, we study the proposed fat sat and MT contrast applied to another SSI sequence, i.e., STFR. The following material starts with a brief overview of the original STFR sequence, and then we discuss the RF spoiling properies and MT contrasts of the proposed FSMT-STFR. Lastly, we demonstrate the proposed methods with simulation studies, phantom experiments and *in-vivo* experiments.

THEORY

Overview of STFR

Figure S-1 shows the proposed FSMT STFR sequence. The original STFR sequence proposed in (1) is the same excluding the FSMT-pulse part (P_0). Compared to SPGR, the main difference of STFR is the tailored tip-up pulse (P_2) at the end of each repetition; this tip-up pulse is tailored to tip up the excited spins back to the longitudinal axis, according to local off-resonance frequencies (1). By adding to the tip-up pulse to restore transverse magnetization, STFR produces high SNR T_2/T_1 contrast images. Another difference of STFR from SPGR is that its net gradient areas between the tip-down excitation and the tip-up pulse have to be zero, so that the spin behaviors are more controllable by the tip-up pulse.

SPGR and STFR have similar RF spoiling properties. For the regular STFR without fat sat, as the net gradient areas in between P_1 and P_2 are zero, the whole part that contains P_1 and P_2 can be treated as a single pulse from the RF spoiling's point of view. Thus, STFR works with the same RF spoiling scheme as SPGR when P_2 keeps the same global RF phase as P_1 (1).

With an additional gradient crusher (P_0) in each repeition, fat sat STFR using the conventional RF spoiling is guaranteed to reach steady state only with perfect fat sat, which is similar to fat sat SPGR. In addition, if P_2 and the nD fat sat pulse are not designed for the whole object, the uncontrolled out-of-slice/slab parts of the object can also produce non-steady-state signals (2). As STFR works with the same RF spoiling when keeping the global phase for P_1 and P_2, we proposed the same adapted RF spoiling scheme for fat sat STFR, and the functions of the global phase of each pulse in STFR also follow the equation [2] in the main paper.

Simultaneous Fat Sat and MTC imaging

Similar to the MT effect sensitivity study for SPGR, we can show that STFR with a MT pulse applied in each repetition also has higher MT effects than using the turbo type MT prep. With the same definitions of MTR and effective MTR as in the main paper, the Appendix of this supplmentary material derives the corresponding function of MTC STFR with respect to MTR:

$$M_z(\text{MTR}) = M_0 \frac{[(1-\text{MTR})E_{1s}^2(1-E_{1f})\cos\alpha + (1+(1-\text{MTR})E_{1s})(1-E_{1s})]}{1-(1-\text{MTR})E_{1s}^2(E_{2f}\sin^2\alpha - E_{1f}\cos^2\alpha)} \qquad \text{[S-1]}$$

where M_0 is equilibrium magnetization, $E_{1s} \triangleq e^{-\frac{T_s}{T_1}}$, T_s is the duration of each gradient crusher, $E_{1f} \triangleq e^{-\frac{T_f}{T_1}}$, $E_{2f} \triangleq e^{-\frac{T_f}{T_2}}$, T_f is the duration between the peak of P_1 and the beginning of P_2, α is the flip angle, and relaxation during tip-up and MT pulse is ignored.

Similar to Fig. 2, Fig. S-2 shows the MT contrast property of MTC STFR. The curves in Fig. S-2 correspond to the same range of T_1 and T_2 values used in Fig. 2, and the sequence was simulated with $T_s = 1$ ms and $T_f = 8$ ms. It is clear that MTC STFR with MT pulses applied in each repetition are much more efficient in producing MT effects than the corresponding turbo MT prep sequence. Such MT sensitivity increases with shorter T_R or longer T_1 and does not change much with different T_2 values. With this property and the same argument for FSMT-SPGR, we proposed to apply the FSMT-

pulse to STFR to produce fat suppression and MT contrast simultaneously, which is called FSMT-STFR sequence.

METHODS AND RESULTS

Simulation: RF Spoiling Schemes

We first show a simulation study on the RF spoiling scheme for fat sat STFR. The simulation setup and parameters were kept the exactly same as the the simulation for SPGR. Fig. S-3 shows the signal evolutions of fat or water when fat-sat STFR is applied with the conventional RF spoiling scheme or the adapted RF spoiling scheme. In all the plots, the sequence with the conventional RF spoiling scheme can not reach steady state (blue solid lines), but the one with the adapted RF spoiling scheme reaches steady state after 100 repetitions at most (red dashed lines).

Phantom Experiment: Fat Sat Pulses

Corresponding to Phantom Experiment II for SPGR, we applied FSMT STFR with the same experiment setup to the same object. It was also compared with the same 5 ms SLR fat sat pulse. According to the corresponding B_0 maps respectively, we designed 2.1 ms long FSMT-pulses with 5 repetitions of 2D spiral-out excitation k-space trajectories, as well as the 2D tailored tip-up pulses (P_2 in Fig. S-1). The adapted RF spoiling scheme was applied to all the sequences. The imaging parameters were kept the same except that T_R were 4.9 ms longer than the corresponding SPGR sequences respectively.

Fig. S-4 shows the results of the experiments, which in general show similar comparison between the FSMT-pulse and the SLR fat sat compared to the results in Fig. 5 for FSMT SPGR. Note that STFR images are less uniform in the oil parts, because the tailored tip-up pulses were designed only for water and have off-resonance effects on fat, making fat suppression more important in STFR imaging. Moreover, although the B_0 maps of these experiments are similar to those of the SPGR experiments, SPGR with SLR fat sat worked well enough for water in both slices, which shows that the fat-sat SPGR is less sensitive to water selection from fat sat pulse than the fat-sat STFR with these particular parameters and object materials .

In-Vivo Experiment: Brain Imaging

Similar to the *in-vivo* experiment I for SPGR, we tested the proposed FSMT-STFR with a brain imaging experiment at 3T. The FSMT-pulse was 2.3 ms long with 7 repetitions of 2D spiral-out trajectories. Using the same experiment setup as for FSMT-SPGR , we applied FSMT-STFR at a superior axial brain slice. The imaging parameters of the STFR sequence were kept the same as in the SPGR experiment except that T_R was 19.1 ms. Fig. S-5 shows the results of this experiment, where FSMT-SPGR suppresses the fat tissue around skulls and attenuates the white matter regions. Specifically, white matter signal is reduced by 50% - 70%.

In-Vivo Experiment: Cartilage Imaging

We then investigated the proposed sequence in the application of cartilage imaging where contrast between synovial fluid and cartilage is desired. Fat suppression is generally beneficial to this application because it can eliminate the surrounding fat that would obscure the tissue of interest (3)(4). MTC is useful for T_2 weighted (5) or T_2/T_1 weighted cartilage imaging (3), where synovial fluid appears brighter than cartilage, so MT can enhance the fluid-cartilage contrast by attenuating cartilage signals.

Therefore, we applied the proposed FSMT-STFR which produces T_2/T_1 contrast (1) to cartilage imaging in human knees. 2D STFR with FSMT-pulse is designed for an axial slice based on a 2D B_0 map acquired with SPGR sequences, and the image data were acquired with 2D spin-warp readout. The FSMT-pulse was 2.1 ms long using 7 repetitions of spiral-out trajectories. One additional image was taken with the FSMT-pulse off as the reference. Other imaging parameters were: slice thickness $= 6$ mm, T_R is 18.5 ms, flip angle $= 16^0$, $a = 117^0$, 1.09 mm$\times 1.09$ mm resolution, FOV = 28 cm $\times 14$ cm.

Fig. S-6 shows the cartilage imaging results comparing the image with no FSMT contrast (middle) to the one with FSMT contrast by the FSMT-pulse (bottom), and the corresponding B_0 map is shown at the top. Fat suppression removed the fat tissue surrounding the cartilage and joint fluid areas and also helped removing the posterior fat that has artifacts due to the tailored tip-up pulse of STFR. In particular, the FSMT-pulse worked very well in the regions with large B_0 inhomogeneity, such as the posterior fat regions. In addition, MT effects suppressed cartilage and muscle signals, and thus highlighted the synovial fluid signals which are pointed out by the red arrows.

APPENDIX

This appendix supplements detailed derivation for equation [S-1]. Referring to Fig.S-1, we calculate the magnetizations at certain time points and each repetition of the sequence is segmented at those time points:

$$\vec{M}_1 \rightarrow P_1 \rightarrow \vec{M}_2 \rightarrow \text{free precession} \rightarrow \vec{M}_3 \rightarrow P_2 \rightarrow \vec{M}_4 \rightarrow C_2 \rightarrow \vec{M}_5 \rightarrow S_1 \rightarrow \vec{M}_6$$

where

$$\vec{M}_1 = \begin{bmatrix} 0 \\ 0 \\ M_z \end{bmatrix}, \vec{M}_2 = \begin{bmatrix} 0 \\ M_z \sin\alpha \\ M_z \cos\alpha \end{bmatrix}$$

After the free precession, there are spin relaxation effects and off-resonance effects, leading to:

$$\vec{M}_3 = \begin{bmatrix} \cos\phi & \sin\phi & 0 \\ -\sin\phi & \cos\phi & 0 \\ 0 & 0 & 1 \end{bmatrix} \begin{bmatrix} \vec{M}_2(1)E_{2f} \\ \vec{M}_2(1)E_{2f} \\ \vec{M}_2(3)E_{1f} \end{bmatrix} + \begin{bmatrix} 0 \\ 0 \\ (1-E_{1f})M_0 \end{bmatrix}$$

where ϕ denotes the phase accumulated due off-resonance effects. If we assume the tip-up pulse is perfectly designed to revert off-resonance effects during the free precession and also have tip-up angle α towards the longitudinal axis, then we have:

$$\vec{M}_4 = \begin{bmatrix} \cos\phi & \sin\phi & 0 \\ -\sin\phi & \cos\phi & 0 \\ 0 & 0 & 1 \end{bmatrix} \begin{bmatrix} 1 & 0 & 0 \\ 0 & \cos\alpha & -\sin\alpha \\ 0 & \sin\alpha & \cos\alpha \end{bmatrix} \begin{bmatrix} \cos\phi & -\sin\phi & 0 \\ \sin\phi & \cos\phi & 0 \\ 0 & 0 & 1 \end{bmatrix} \vec{M}_3$$

Then if the crusher C_2 perfectly removes the transverse magnetization, we then have:

$$\vec{M}_4 = \begin{bmatrix} 0 \\ 0 \\ E_{1s}\vec{M}_4(3) + (1-E_{1s})M_0 \end{bmatrix}$$

After C_2, we consider the overall effect of S_1 as having a change in the z magnetization due to MTR and T_1 relaxation. Hence, we have:

$$\vec{M}_6 = \begin{bmatrix} 0 \\ 0 \\ (1 - \text{MTR})\vec{M}_5(3)E_{1s} + (1 - E_{1s})M_0 \end{bmatrix}$$

When the sequence reach a steady state, we have $\vec{M}_6 = \vec{M}_1$ or $\vec{M}_6(3) = M_z$. Then the steady-state longitudinal magnetization of MTC STFR prior to each P_1 can be expressed as a function of MTR, which is equation [S-1].

References

1. Nielsen JF, Yoon D, Noll DC. Small-tip fast recovery imaging using non-slice-selective tailored tip-up pulses and radiofrequency-spoiling. Magnetic Resonance in Medicine 2013;69:657–666.

2. Zhao F, Nielsen JF, Noll DC. Fat saturation for 2D small-tip fast recovery imaging using tailored 3D spectral-spatial pulses. In Proceedings of the 21th Scientific Meeting of International Society for Magnetic Resonance in Medicine, Salt Lake City. 2013; 252.

3. Gold GE, Reeder SB, Yu H, Kornaat P, Shimakawa AS, Johnson JW, Pelc NJ, Beaulieu CF, Brittain JH. Articular cartilage of the knee: Rapid three-dimensional MR imaging at 3.0 t with ideal balanced steady-state free precession—initial experience1. Radiology 2006;240:546–551.

4. Disler DG, McCauley TR, Wirth CR, Fuchs MD. Detection of knee hyaline cartilage defects using fat-suppressed three-dimensional spoiled gradient-echo mr imaging: comparison with standard mr imaging and correlation with arthroscopy. American journal of roentgenology 1995;165:377–382.

5. Lang P, Noorbakhsh F, Yoshioka H. Mr imaging of articular cartilage: current state and recent developments. Radiologic Clinics of North America 2005;43:629–639.

FIGURES

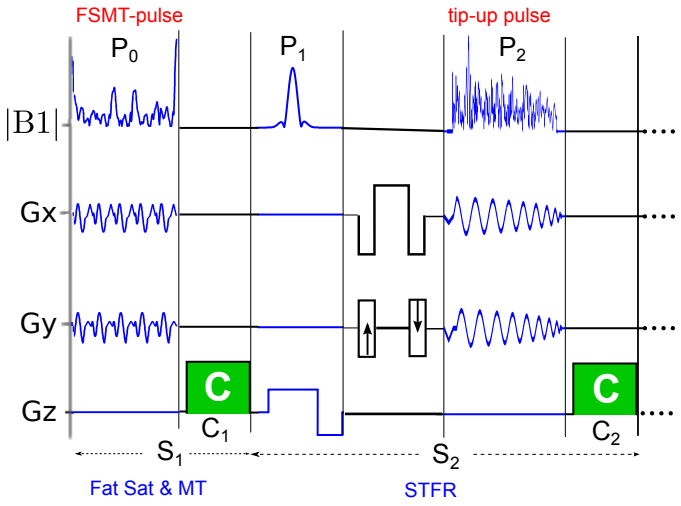

Figure S-1: Illustration of the 2D version of the proposed FSMT-STFR sequence.

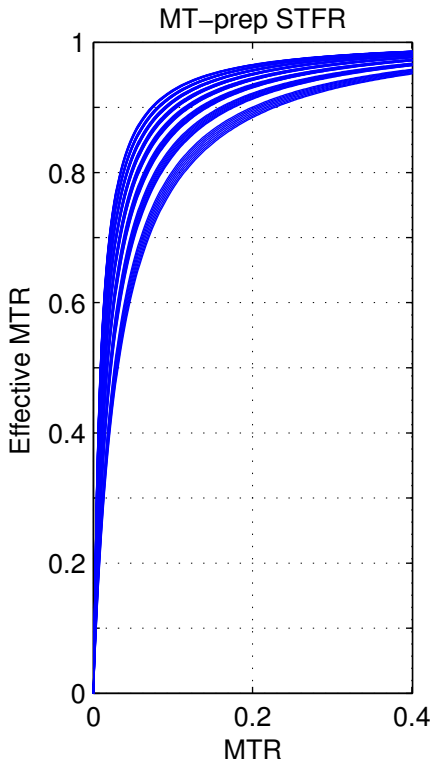

Figure S-2: Plots of the effective MTR in terms of MTR for MTC STFR; The plots are from all the combinations of the following relaxation parameters: $T_1 = [0.5, 0.7, \ldots, 1.7, 1.9]$ s, and $T_2 = [50, 70, \ldots, 170, 190]$ ms. STFR is sensitive to small magnetization attenuation caused by MT effect.

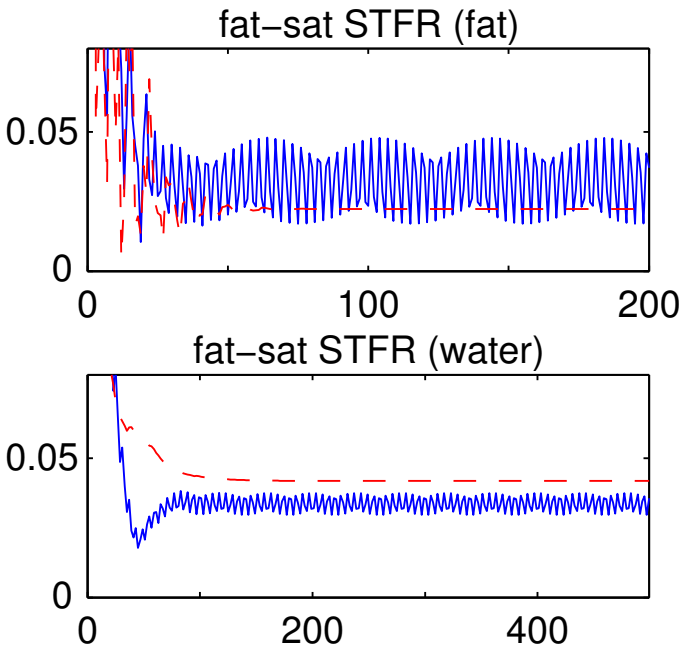

Figure S-3: Signal evolutions of fat spin (upper row) and water spin (lower row) using fat-sat STFR with different RF spoiling schemes. Both longitudinal axes denote the ratio between the transverse magnetization right after P_1 and the magnetization at equilibrium, M_{xy}/M_0; the horizontal axes denote the number of repetitions. The signal reaches steady state with the adapted RF spoiling scheme (dashed lines), but not with the conventional RF spoiling scheme (solid lines).

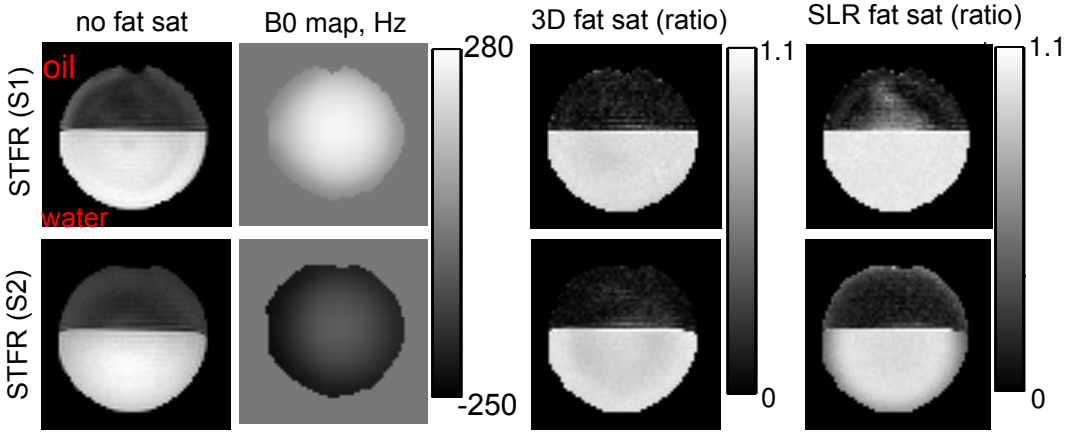

Figure S-4: The results of the phantom experiments for testing fat-sat STFR where we picked two representative slices for each sequence. From left to right, 1st column: the original images with no fat sat (oil on top of water), 2nd column: B_0 maps, 3rd column: the ratio images with the 3D fat sat pulse, 4th column: the ratio images with the SLR fat sat pulse. The ratio image is calculated by taking the ratio between the image with fat sat and the corresponding image without fat sat.

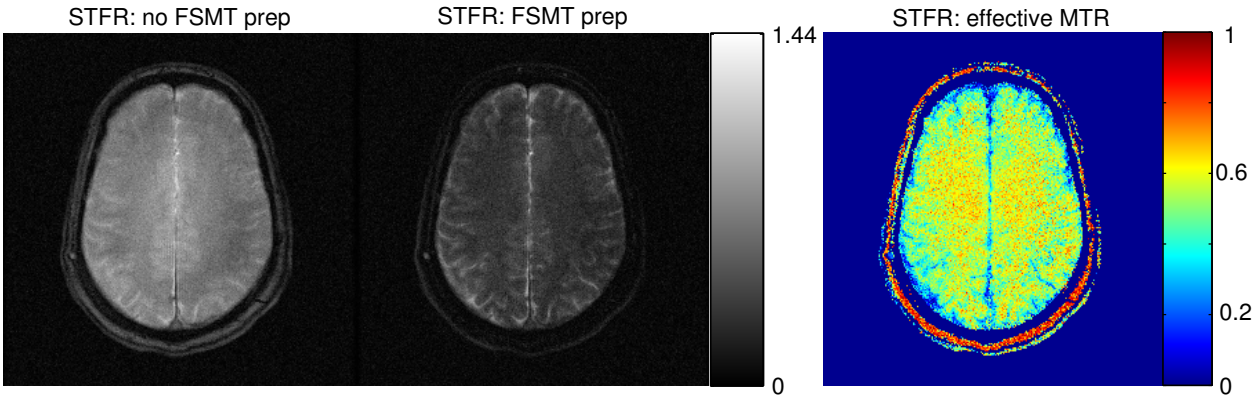

Figure S-5: STFR images acquired in the *in-vivo* experiments on human head. Left: without FSMT contrast; middle: with FSMT contrast; right: effective MTR maps. The left two images have the same gray scale.

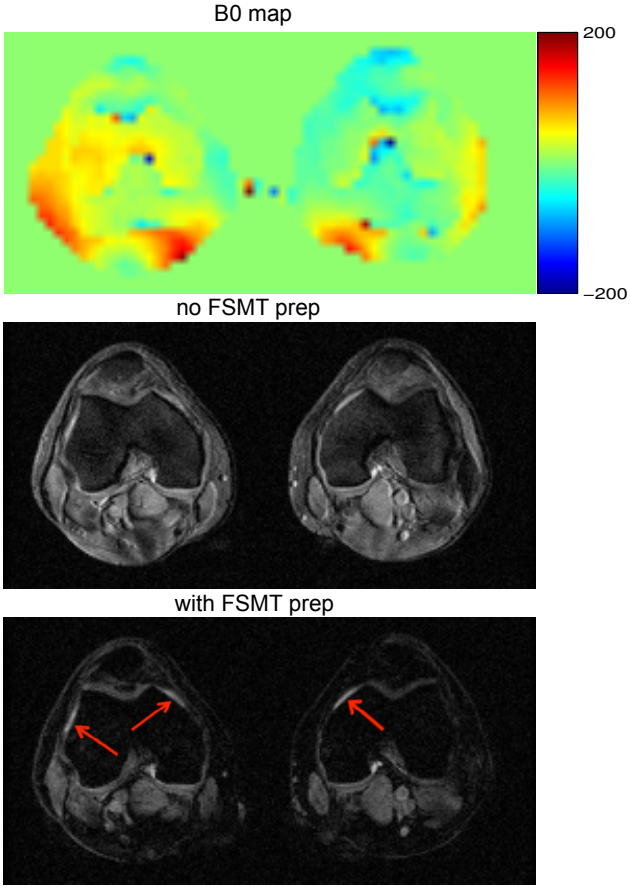

Figure S-6: The resulting STFR images of the cartilage imaging and the corresponding B_0 map (top). The image with no FSMT-pulse is at the middle, and the image with FSMT-pulse is at the bottom. These two images are in the same gray scale. The red arrows point to synovial fluid which is highlighted better in the image with simultaneous fat suppression and MTC.